Journal of Gerontology: BIOLOGICAL SCIENCES
2002, Vol. 57A, No. 7, B270–B278

Age-Associated Cardiomyopathy in Heterozygous Carrier Mice of a Pathological Mutation of Carnitine Transporter Gene, *OCTN2*

Xiaofei E,[1] Yasuhiko Wada,[1,2] Miwako Dakeishi,[1] Fujiko Hirasawa,[1] Katsuyuki Murata,[1] Hirotake Masuda,[3] Toshihiro Sugiyama,[4] Hiroko Nikaido,[5] and Akio Koizumi[1,6]

Departments of [1]Hygiene, [3]Pathology 2, and [4]Biochemistry, Akita University School of Medicine, Japan.
[2]Department of Hygiene, Hyogo College of Medicine, Nishinomiya, Japan.
[5]Institute for Experimental Animals, Faculty of Medicine, Kanazawa University, Japan.
[6]Department of Health and Environmental Sciences, Kyoto University School of Public Health, Japan.

The purpose of this study was to test whether heterozygotes of juvenile visceral steatosis mice, a model for systemic carnitine deficiency, may develop age-associated cardiomyopathy. Tissue morphological observations were carried out by light and electron microscopy to compare the heterozygous and age-matched control mice at periods of 1 and 2 years. Possible effects of the pathological mutation on lipid and glucose levels was also evaluated in humans and mice. Except mild increases in serum cholesterol levels in male heterozygous mice and humans, no changes were found in other factors, indicating that none of the confounding factors seems to be profound. Results demonstrated that heterozygous mice had larger left ventriclular myocyte diameters than the control mice. Morphological changes in cardiac muscles by electron microscopy revealed age-associated changes of lipid deposition and abnormal mitochondria in heterozygous mice. Two out of 60 heterozygous cohort and one out of nine heterozygous trim-kill mice had cardiac hypertrophy at ages older than 2 years. The present study and our previous work suggest that the carrier state of *OCTN2* pathological mutations might be a risk factor for age-associated cardiomyopathy.

CARNITINE is a carrier of free fatty acids into mitochondria for β-oxidation (1). Shortages in carnitine result in impaired fuel utilization in β-oxidation and cause cellular pathology in various organs such as the kidneys, heart, and central nervous system. In addition, mild, chronic shortage is suspected to cause cardiac hypertrophy in humans in concert with physiological aging (1). Engel and Angelini first described systemic carnitine deficiency (SCD), detailing the varied clinical, morphologic, biochemical, and metabolic features of this autosomal recessive disorder, in 1973 (2). It is characterized by progressive cardiomyopathy, skeletal myopathy, hypoglycemia, and hyperammonemia. At least two SCD clinical phenotypes have been reported (3).

We have previously shown by linkage analysis that a locus on 5q31 is responsible for SCD (4). We further demonstrated that mutations of *OCTN2*, which has carnitine transporter function (5), cause SCD (6). The impaired transporter function leads to reduced intestinal and renal reabsorption of carnitine, resulting in low carnitine levels in the body. As a result of incomplete β-oxidation, shortages in adenosine triphosphate (ATP) supply occur in various organs such as the heart, nervous system, liver, and skeletal muscle; the shortages cause a variety of clinical symptoms, including Reye's syndrome (7).

Population-based genetic epidemiology shed new light on some aspects of SCD (1). First, the population prevalence of *OCTN2* mutations was reported to be as high as 1 out of 252 chromosomes. Second, SCD was directly shown to be a cause of sudden infant death. Third, heterozygotes of *OCTN2* mutations were shown to be prone to late-onset cardiac hypertrophy. The last observation was unexpected and particularly important, because carriers of mutated disease genes are usually free of symptoms.

The prevalence of cardiomyopathy, which is clinically manifested as left ventricular hypertrophy (LVH), increases markedly with aging, approaching one third in men and one half in women 70 years or older (8); however, its pathogenesis remains largely unknown. The grave consequences of LVH have been well documented and the following potential sequelae of LVH have been identified: myocardial ischemia and infarction, ventricular arrhythmias, heart failure with a preserved or impaired left ventricular systolic function, cerebrovascular disease, and cardiovascular mortality. The high prevalence rate of LVH in the elderly population underscores the urgent need to adopt strategies that help to prevent the development of LVH.

A reasonable hypothesis from the previous genetic epidemiology study (1) suggests that *OCTN2* mutations may be

one of the risk factors for age-associated cardiac hypertrophy. The juvenile visceral steatosis (JVS) mouse is a model for SCD (9). The JVS mouse, derived from the C3H.OH strain, shows similar characteristics of SCD in humans. A mutation search of the *OCTN2* gene of JVS mice revealed a missense mutation, CTG (Leu) to CGG (Arg), at codon 352 located within the sixth transmembrane domain (10), which disrupts carnitine transport activity (11).

The aim of the present study was twofold. First, we tested whether mutation of *OCTN2* is a risk factor for cardiomyopathy in JVS heterozygotes during aging. Pathological studies were conducted on the heart at various ages. Using genetically homogeneous mice, with the exception of the *OCTN2* mutation, enabled us to pinpoint effects of *OCTN2* mutation on the heart. Second, if carnitine levels are low, there may be a possibility that lipid and glucose metabolism is perturbed because carnitine is the essential carrier of fatty acids. It is well known that impaired lipid and glucose metabolism is a confounding factor for cardiac hypertrophy in the elderly population (12–14). We thus determined glucose and lipid metabolisms in mice and lipid metabolism in humans.

Methods

Human Volunteers and Population Prevalence of Carriers of OCTN2 Mutations

Participants, aged 20–48 years, were volunteers from a group of people who attended the annual health examination program sponsored by City A in the northern part of Akita Prefecture. Some 4500 individuals participated in the study and provided written informed consent for a search for Trp132X and Ser467Cys mutations. The expected population prevalence of carriers of the two pathological mutations, which were estimated from our previous genetic epidemiological study (1) on a population in another city in Akita, 40 miles west of City A, were 1:324 and 1:243, resulting in a population prevalence of deleterious mutation of 0.72% (1:139). Informed consent was also obtained from all participants for body weight (BW), total cholesterol, triglyceride (TG), body mass index (BMI), and high-density lipoprotein (HDL) cholesterol measurements.

DNA was extracted from peripheral blood samples. The Trp132X mutation, which is in exon 2 of the *OCTN2* gene, disrupts the *NlaIV* restriction site in exon 2. The Ser467Cys mutation, which is in exon 8 of the *OCTN2* gene, creates a *PvuII* restriction site. A polymerase chain reaction (PCR) was conducted as previously reported, using primers sets to obtain products covering exon 2 and exon 8 (1). PCR products were subjected to restriction enzyme digestion with the corresponding enzymes. This study was conducted under the guidelines approved by the Ethical Committee of Akita University School of Medicine.

Animals

JVS heterozygous male (+/−) and female mice (+/−), which originally derived from the C3H mouse strain (15), were provided by the Institute for Experimental Animals, School of Medicine, Kanazawa University, Japan (15). All mice were handled in accordance with the Animal Welfare Guidelines of Akita University (1990). Heterozygous female and male mice were mated to obtain offspring. The offspring were genotyped by PCR 6 weeks after birth. The four groups, male control (+/+; MCt), male heterozygote (+/−; MHet), female control (+/+; FCt), and female heterozygote (+/−; FHet), were investigated in this study. They were maintained as cohort (30 mice in the group) or trim-kill groups (100 mice/group, sacrificed at 6 months, 1 year, or 2 years of age). Mice were housed in cages with wood shavings, a relative humidity of 50%, and a 12-hour light (7 AM–7 PM)–12-hour dark (7 PM–7 AM) photocycle. They were given free access to food (Commercial Lab Food CE-2, Nippon Clea, Tokyo, Japan) and water. The CE-2 diet contains (percentage of weight per weight) fat (4.4%), protein (24.8%), carbohydrate (51.6%), and total energy at 1445 J/100 g of diet.

Genotyping

DNA for genotyping was isolated from blood (20–50 μl) collected from the tail vein. A PCR was conducted in a reaction mixture containing 50mM Tris(hydroxymethyl)aminomethane, pH 9.5, 20mM ammonium sulfate, 1.5mM magnesium chloride, 1mM of each primer, 50 ng of genomic template, 1.5 U of Tag Gold polymerase (Perkin-Elmer Corp., Branchburg, NJ), and 300μM of each deoxynucleoside 5′-triphosphate, in a final reaction volume of 15 μl. PCR amplification was performed in an MJ Research PTC-100 thermal cycler (Watertown, MA), using a program at 95°C for 9 minutes followed by 40 cycles (94°C for 45 seconds, 57°C for 45 seconds, and 74°C for 1 minute) and the last extension of 72°C for 7 minutes with the following primers: forward primer, 5′-GAGCCCAGGGAAACTTAACT-3′; reverse primer, 5′-AAAATAGCCCACTGATATGGT-3′. The PCR product was digested with 1.5 units of *Aci I* for 16 hours at 37°C. The L352R mutation, a single base substitution (T → G) at codon 352, creates an *Aci I* restriction site. Whereas wild type DNA (T/T) gave a single band at 205 bp, DNA from heterozygotes (T/G) gave two bands at 205 bp (normal allele) and 181 bp (mutant allele; see Figure 1).

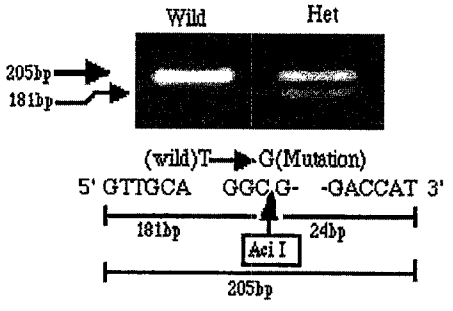

Figure 1. Mice were examined for their genotype, with a polymerase chain reaction (PCR) combined with restriction fragment length polymorphism analysis, for the T → G mutation; *Aci I* was used to digest PCR products. The arrows indicate the fragment derived from the wild type allele 205 bp (uncleaved) and mutant allele-derived fragments (181 bp).

Glucose Metabolism

An intraperitoneal glucose tolerance test was determined for each group (6 months, 1 year, and 2 years) 1 week before sacrifice. Mice, fasted overnight (~16 hours), were injected intraperitoneally with glucose (1 ml/kg of a 15% solution). Blood glucose levels were determined in blood collected from the tail vein by using a TIDE monitor (Miles-Sankyo, Tokyo, Japan). Determinations were made before glucose injection and 30, 60, and 120 minutes afterward. BWs of the cohort group were measured regularly between 4 PM and 5 PM once a month. BW for trim-kill groups was measured just prior to sacrifice with pentobarbital (50 mg/kg) after a 16-hour fast.

Autopsy and Light Microscopy

One-milliliter blood samples were collected from the aorta abdominalis and allowed to clot to obtain serum. The heart and both kidneys were isolated immediately and weighed. The tissues were fixed in 10% buffered formalin (pH 7.4). Paraffin sections were stained with hematoxylin-eosin and Azan methods for light microscopy. The transverse areas of the left and right ventricular walls and septum were examined under 20× magnification with a Video Meter (Olympus, BX50, Tokyo, Japan, and Hi Vision Filing System, Tokyo, Japan) (16). The diameters of myocytes in the left and right ventricular walls and intraventricullar septum were determined in stained cross-sectional areas by measuring the shortest diameter at the level of the nucleus of 50 myocardial fibers, using an ocular micrometer at 400× magnification (17).

Electron Microscopy

Five cardiac tissues from each group were processed for electron microscopic observations. Samples were immediately cut into small pieces after removal and fixed with 3% glutaraldehyde solution in 0.1M cacodylate buffer (pH 7.4) for 4 hours to overnight at 4°C. After postfixation with 1% osmium tetroxide solution buffered at pH 7.4 with 0.1M cacodylate phosphate buffer for 2 hours at 4°C, specimens were dehydrated with degraded alcohol (70%–100%) and embedded in Epon. Ultrathin sections, cut on a BROMMA-LKB 2088 ultramicrotome (Sankyo Ltd., Tokyo, Japan), were stained with osmiun tetraoxide solution, uranyl acetate, and lead citrate, and they were then observed with an electron microscope (JEOL JEM-1200EX, Nihon Koden, Tokyo, Japan).

Biochemical Analysis

Parts of the heart and kidney (usually 0.05–0.1 g) were excised and homogenized with 10 vol of distilled water. All subsequent steps were performed at 4°C. The homogenate was deproteinized with 1/5 vol of 30% percholoric acid and centrifuged for 5 minutes. The resulting supernatant was neutralized with 1N potassium hydroxide. The L-carnitine levels in serum and tissue were then measured by the enzymatic cycling technique with reduced nicotinamide adenine dinucleotide, thio-nicotinamide adenine dinucleotide, and carnitine dehydrogenase, using a free Carnitine Kit (Kainos Co., Tokyo, Japan).

Serum concentrations of total cholesterol and TGs in mice and humans were measured by enzymatic methods, using commercial kits from Wako (Wako Co., Osaka, Japan). HDL cholesterol was also determined with a commercially available kit (HDL-C Wako) by a method after selective precipitation of apo B-containing lipoproteins (18).

Statistic Analysis

Results are expressed as means ± *SD*s. A statistical analysis was performed with an analysis of variance (ANOVA) with repeated measurements or analysis of covariance (ANCOVA) to control for age and sex. Differences between the two groups were tested by unpaired Student's *t* tests. Survival curves were calculated by using the Kaplan–Meier method (19). A log rank test was done for comparing survival rates. A value of $p < .05$ was considered to be statisti-

Table 1. Comparison of Serum Lipid Levels in Controls and Heterozygotes for Humans and Mice

	Total Cholesterol (mg/dl)		BMI (kg/m²)		Triglyceride (mg/dl)		HDL Cholesterol (mg/dl)	
Sex	Control	Heterozygote	Control	Heterozygote	Control	Heterozygote	Control	Heterozygote
Male			Humans					
≤35 y	157.2 ± 30.7(10)	169.2 ± 92.6(6)	23.3 ± 1.6(10)	22.7 ± 1.8(6)	83.3 ± 24.6(10)	96.7 ± 26.8(6)	52.0 ± 12.2(10)	50.0 ± 12.5(6)
>35 y	186.7 ± 25.9(10)	224.4 ± 25.8(7)‡**	23.6 ± 1.6(10)	22.8 ± 1.5(7)	96.0 ± 36.0(10)	83.9 ± 24.7(7)	46.8 ± 11.9(10)	53.0 ± 11.7(7)
Female								
≤30 y	141.4 ± 27.1(8)	150.8 ± 27.0(5)	21.3 ± 0.8(8)	21.4 ± 1.1(5)	82.6 ± 24.7(8)	77.8 ± 26.0(5)	60.5 ± 9.3(8)	57.0 ± 12.5(5)
>30 y	172.1 ± 26.5(12)	202.5 ± 37.0(6)	22.3 ± 1.4(12)	21.9 ± 1.1(6)	101.7 ± 48.5(12)	112.3 ± 38.8(6)	56.3 ± 13.0(12)	56.0 ± 11.3(6)
Male			Mice†					
6 mo	115.8 ± 8.9(9)	110.3 ± 10.6(10)	29.6 ± 2.6(9)	30.2 ± 2.8(10)	116.5 ± 35.8(9)	83.2 ± 25.6(10)‡*		
1 y	115.3 ± 9.3(5)	125.0 ± 7.9(9)	31.5 ± 1.1(5)	33.4 ± 3.0(9)	105.4 ± 17.8(5)	118.3 ± 37.0(9)		
2 y	105.6 ± 16.4(5)	127.1 ± 14.6(8)‡*	31.2 ± 3.1(5)	30.1 ± 3.3(8)	66.9 ± 19.9(5)	73.7 ± 33.8(8)		
Female								
6 mo	82.0 ± 11.2(10)	90.3 ± 11.3(10)	23.1 ± 2.1(10)	23.8 ± 2.1(10)	68.7 ± 22.4(10)	65.6 ± 13.2(10)		
1 y	93.3 ± 18.0(8)	86.4 ± 7.0(10)	29.8 ± 7.6(8)	26.4 ± 1.5(10)	111.0 ± 37.6(8)	117.1 ± 22.3(10)		
2 y	96.4 ± 15.0(7)	107.5 ± 13.7(7)	25.4 ± 3.9(7)	26.3 ± 1.3(7)	67.7 ± 21.0(7)	88.6 ± 20.7(7)		

Notes: Results are expressed as mean ± *SD*, with numbers in parentheses. BMI = body mass index; HDL = high-density lipoprotein.

†Body weight (g) is used, instead of BMI (kg/m²), for mice.

‡By *t* test; differences with a value of $p < .05$ were considered significant.

*$p < .05$; **$p < .01$.

cally significant. These analyses were performed by using SAS software (SAS Institute Inc., Cary, NC).

Results

Characterization of Human Heterozygotes in Terms of Lipid Metabolisms

Fourteen carriers of Trp132X and 9 carriers of Ser467 Cys were found, giving a total of 23 carriers among the 4500 participants. From this the population prevalence was calculated to be 1:196 (0.5%). The levels of total cholesterol, TG, BMI, and HDL cholesterol were measured in 40 wild type people (20 men and 20 women) and 24 heterozygous people (13 men and 11 women) with *OCTN2* mutation from a population from the Akita Prefecture in Japan. There was a significant difference in cholesterol levels for humans with age (>35 years vs ≤35 years; $p < .001$; ANOVA) and genotype ($p < .001$; ANOVA).

An ANCOVA to control for age and sex was used for comparing cholesterol levels by genotype difference. The cholesterol level was significantly elevated in the people with an *OCTN2* mutation (heterozygotes, 189.8 ± 38.3, $n = 24$; wild type, 165.9 ± 31.1, $n = 40$). When the data were classified by age (≤35 years or >35 years), and when Student's t tests were used, there was a significant difference in levels ($p < .01$; t test) among men over the age of 35 (wild type = 186.7 ± 25.9, $n = 10$; Heterozygotes = 224.4 ± 25.8, $n = 7$; Table 1). Although there was no significant difference in cholesterol levels in men younger than 35 years of age, there was a tendency toward higher levels for heterozygotes (157.2 ± 30.7, $n = 10$; 169.2 ± 92.6, $n = 6$).

Lipid and Glucose Metabolisms in Heterozygous Mice

In mice, a similar trend was confirmed in lipid metabolism: Cholesterol levels in M Het were significantly higher than in MC+ (Table 1). In contrast, however, only an increased tendency was seen in F Het mice (107.5 ± 13.7, $n = 7$) compared with FC+ (96.4 ± 15.0, $n = 7$). There was no significant difference in the cholesterol levels of mice at 6 months and 1 year.

In terms of glucose metabolism, there was no significant difference in blood glucose levels between control and heterozygous JVS mice (data not shown). Therefore, it can be concluded that glucose metabolism is not impaired in heterozygous mice.

The free carnitine content in the myocardium of heterozygous JVS mice was approximately 75% of the control mice at 6 months, 1 year, and 2 years of age; 686.9 ± 119.0, 438.1 ± 105.5, and 740.2 ± 85.3 in heterozygotes, respectively; 952.4 ± 155.0, 570.0 ± 150.8, and 967.5 ± 64.2 nmol/g in control mice, respectively. The level of free carnitine was also significantly reduced in heterozygous mice at 1 and 2 years, but not at 6 months, of age in the serum (78.4% of control) and at all ages in the kidney (70.5% of control).

Survival Rate

There were no differences in BW levels between heterozygotes and control mice in either sex. Male heterozygous and control mice reached maximum mean BW level, 35 g ± 5, at 8 months, and they maintained that weight until 18 months, at which time it gradually decreased until 24 months to a mean of 30 g ± 3 (data not shown). The growth rate of female heterozygotes and controls reached mean plateau levels (27 ± 3 g for both groups) at 6 months, and this weight was maintained until 24 months of age (data not shown).

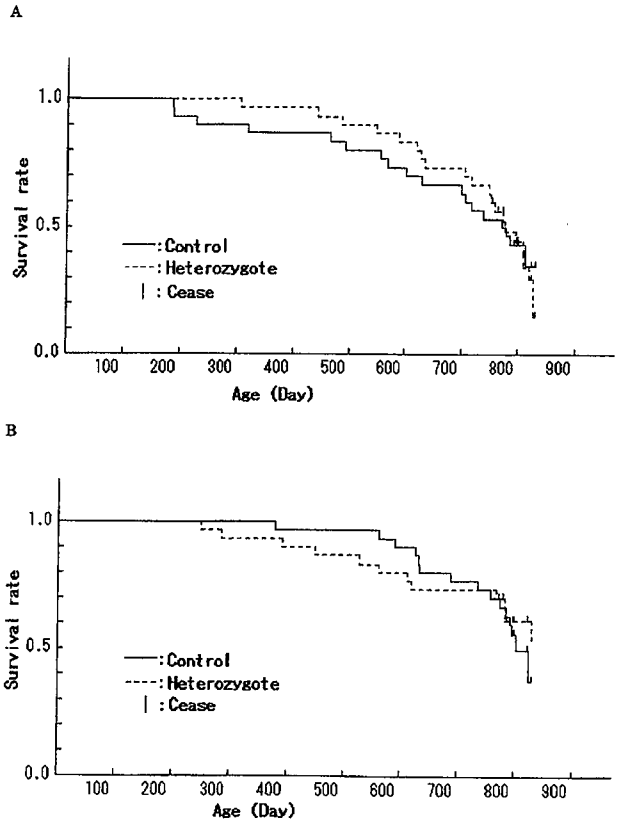

Figure 2. Survival rates of cohort mice for four groups—female control, female hetyerozygote, male control, and male heterozygote. Initial numbers of each group were 30. Survival rates expressed by the Kaplan–Meier method were not significantly different from genotype for female (**A**) and male (**B**) mice separately ($p > .05$).

The gross survival rates, which include all mortalities regardless of cause, is summarized in Figure 2 (A, female mice; B, male mice). There was no significant difference in mortality rates between control and heterozygous mice at 829 days of age ($p > .05$, Kaplan–Meier method).

Autopsies of cohort dead mice revealed that one female mouse (773 days) and one male mouse (829 days) had cardiac hypertrophy as indicated by the ratios of heart weight/BW, 8.5×10^{-3} and 8.4×10^{-3}, respectively, which is approximately 1.7 times that of other dead cohort mice ($5 \times 10^{-3} \pm 1 \times 10^{-3}$). As a result of tissue degeneration, the tissues from these mice with cardiac hypertrophy were not examined by electron microscopy. The autopsies revealed that 74% of dead male mice, heterozygotes and controls (20 out of 27), and 83% of dead female mice, heterozygotes and

Table 2. BW, HW, HW/BW Ratio, and the Areas of Both Ventricles and Septum for Control and Heterozygous JVS Mice

Parameter	6 mo		1 y		2 y	
	Control	Heterozygote	Control	Heterozygote	Control	Heterozygote
BW (g)						
Male	29.6 ± 2.6(9)	30.2 ± 2.8(10)	31.5 ± 1.1(5)	33.4 ± 3.0(9)	31.2 ± 1.8(5)	30.1 ± 3.3(8)
Female	23.1 ± 2.1(10)	23.8 ± 2.1(10)	29.8 ± 7.6(8)	26.4 ± 1.5(10)	25.4 ± 3.9(7)	26.3 ± 1.3(7)
HW (g)‡*						
Male	0.11 ± 0.01(9)	0.12 ± 0.01(10)	0.13 ± 0.01(5)	0.14 ± 0.03(9)	0.12 ± 0.00(5)	0.12 ± 0.01(8)
Female	0.09 ± 0.01(10)	0.10 ± 0.01(10)	0.10 ± 0.01(8)	0.10 ± 0.01(10)	0.11 ± 0.00(7)	0.10 ± 0.01(7)
HW/BW ($\times 10^{-3}$)						
Male	3.6 ± 0.3(9)	3.9 ± 0.4(10)	4.1 ± 0.3(5)	4.0 ± 0.6(9)	3.8 ± 0.1(5)	4.1 ± 0.2(8)
Female	3.9 ± 0.4(10)	4.0 ± 0.3(10)	3.5 ± 0.5(8)	3.7 ± 0.3(10)	4.0 ± 0.6(5)	4.1 ± 0.2(7)
Ventricular walls and septum (mm^2)						
Male	13.66 ± 1.17(5)	14.0 ± 1.25(5)	13.64 ± 0.54(5)	14.24 ± 1.45(5)	15.83 ± 0.76(5)	15.33 ± 0.87(5)
Female	11.82 ± 0.80(5)	11.67 ± 0.92(5)	11.22 ± 0.88(5)	11.16 ± 0.46(5)	14.04 ± 1.82(5)	14.47 ± 1.45(5)

Notes: Results are expressed as mean ± *SD*, with number in parentheses. BW = body weight; HW = heart weight; JVS = juvenile visceral steatosis.
‡By two-way analysis of variance; differences with a value of $p < .05$ were considered significant.
*$p < .05$ (only at 6 mos).

controls (31 out of 37), had tumors (data not shown). No deaths specific to genotype, including tumor death, were found.

Effects of OCTN2 Mutation on Heart in Mice

BW, heart weight, the ratio of heart weight/BW, and the areas including the wall of both ventricles and septum in transverse section were summarized for control and heterozygous mice at 6 months, 1 year, and 2 years of age (Table 2). There were no significant differences between controls and heterozygotes ($p > .05$; ANOVA) for BW, heart weight, and the wall areas of both ventricles and septum at 6 months, 1 year, and 2 years of age (except for heart weight at 6 months, which is $p < .05$; ANOVA).

The myocyte diameter in the left ventricles of heterozygous mice was significantly larger than that of control mice for all 6-month-old, 1-year-old, and 2-year-old mice, as shown in Figure 3 (genotype, $p < .01$; age, $p < .0001$; gender, $p < .01$; ANOVA). A significant difference of myocyte diameter in the left ventricle was also observed (16.9 ± 1.3 μm vs 17.8 ± 1.2 μm) when a comparison was done between control and heterozygous mice by an ANCOVA to control for age and gender. At 2 years, myocyte diameter in the left ventricular walls of heterozygous mice was increased approximately 6.6% with respect to control mice (18.9 ± 0.8 μm vs 17.7 ± 1.7 μm; $p < .05$; ANOVA). No significant difference for myocyte diameter was seen in the right ventricular wall and interventricular septum between control and heterozygous mice.

Pathological findings revealed by electron microscopy of cardiac muscle in 1-year-old and 2-year-old mice are shown in Table 3 (no observations for 6-month-old mice). Progressive damage of interfibrillar mitochondria (IFM) were found in almost all of both male and female heterozygous 2-year-old mice. In female mice, there was more extensive lipid droplet accumulation in heterozygotes. Moreover, as age increased, the number and density of lipid droplets also increased. In heterozygous mice, cardiac muscle cells showed an increase in the numbers of IFM and perinuclear mitochondria. Bundles of myofibrils appeared to be distorted or split; these abnormal structures were not seen in most of control mice.

When the mice were 1 year of age, lipid droplets could more frequently be found in both male and female heterozygous mice (Figures 4B and 4D) compared with the age-matched controls (Figures 4A and 4C). Partially or completely digested swollen mitochondria with disrupted cristae were seen in 2-year-old heterozygous mice (Figures 4F and 4H). The 2-year-old control mice also showed a mild abnormal tendency (Figures 4E and 4G) compared with the 1-year-old control mice (Figures 4A and 4C). In addition, membranous whorls and vacuoles as well as cytoplasmic vacuolization could be found in some myocytes of heterozygotes (data not shown).

One out of nine male heterozygous mice with cardiac hypertrophy was found in the trim-kill group at 2 years of age. The ratio of heart weight/BW was 5.4×10^{-3} compared with the control value of $3.7 \times 10^{-3} \pm 5 \times 10^{-4}$. Microscopic examination revealed an increase in cardiac cell volume with deformation and enlargement of the nucleus (data not shown). Electron microscopic examination revealed

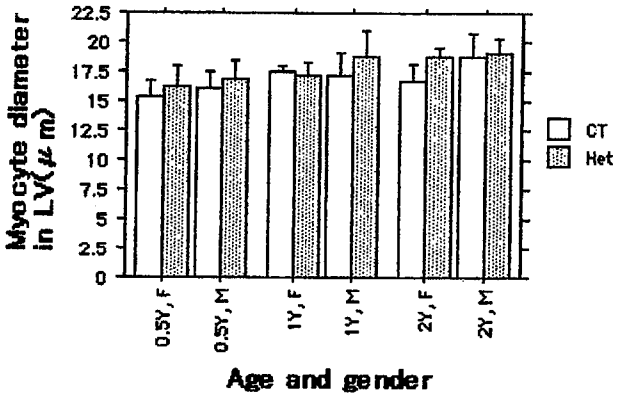

Figure 3. The myocyte diameter in the left ventricle (LV) of control (CT) and heterozygous (Het) mice at 0.5, 1, and 2 years of age. Data are mean ± *SD*. The differences among genotype, age, and gender were analyzed by a three-way analysis of variance with repeated measures: genotype, $p < .01$; age, $p < .0001$; gender, $p < .01$.

Table 3. Summary of the Pathological Findings Revealed by Electron Microscopy in 1- and 2-Year-Old Control and Heterozygous JVS Mice

Age	Sex	Genotype	Lipid Droplets	Increase in IFM No.	IFM Damage	Increase in SSM No.	SSM Damage	BMF Damage	Increase in PNM No.
1 y	F	Ct	±	—	—	—	—	—	—
1 y	F	Ct	—	—	—	—	—	—	—
1 y	F	Ct	±	—	—	—	—	—	—
1 y	F	Ct	—	—	—	—	—	—	—
1 y	F	Ct	±	—	—	—	—	—	—
1 y	F	Het	++	++	±	—	—	+	++
1 y	F	Het	+	±	±	—	—	±	—
1 y	F	Het	±	±	±	—	—	±	±
1 y	F	Het	+	±	+–++	—	—	+	—
1 y	F	Het	+	+	+	—	—	±	±
1 y	M	Ct	—	—	—	—	—	—	—
1 y	M	Ct	—	—	—	—	—	—	—
1 y	M	Ct	—	—	—	—	—	—	—
1 y	M	Ct	—	—	—	—	—	—	—
1 y	M	Ct	—	—	—	—	—	—	—
1 y	M	Het	+	±	±	±	—	+	++
1 y	M	Het	—	++	++	++	+	++	+
1 y	M	Het	+	±	+–++	—	±	—	±
1 y	M	Het	++	+	±	±	—	±	+
1 y	M	Het	±	+	+	±	—	+	+
2 y	F	Ct	—	—	±	—	±	—	—
2 y	F	Ct	—	—	—	—	—	—	—
2 y	F	Ct	—	—	—	—	—	—	—
2 y	F	Ct	—	—	±	—	—	±	±
2 y	F	Ct	±	—	±	—	—	±	—
2 y	F	Het	++–+++	+	++	—	—	+	++
2 y	F	Het	±	—	+	—	—	—	—
2 y	F	Het	±	±	+	—	±	—	+
2 y	F	Het	+–++	—	++	—	—	±	—
2 y	F	Het	+++	—	+–++	—	—	+	—
2 y	M	Ct	—	—	—	—	—	—	±
2 y	M	Ct	—	—	±	—	—	—	—
2 y	M	Ct	—	—	—	—	—	—	—
2 y	M	Ct	±	—	±	—	±	—	—
2 y	M	Ct	—	—	±	—	—	—	—
2 y	M	Het	±	±	+–++	—	±	±	±
2 y	M	Het	—	—	+	—	±	±	—
2 y	M	Het	—	+	++	+	—	++	±
2 y	M	Het	—	+–++	+–++	—	—	+	++–+++
2 y	M	Het	—	—	+–++	—	±	±	—

Notes: IFM = interfibrillar mitochondria; SSM = subsarcolemmal mitochondria; BMF = bundles of myofibrils; PNM = perinuclear mitochondria; JVS = juvenile visceral steatosis; M = male; F = female; Ct = control; Het = heterozygote. Under the magnification of 4000×, five randomly selected fields were observed. In control mice, 100 ± 30 mitochondria/field and 20 ± 5 bundles of myofibrils were found, irrespective of age. To evaluate the increase in numbers of mitochondria, we assumed 100 mitochondria/field as a control. The extent of increase was graded as follows: normal (—) <10%, very mild (±) 10–20%, mild (+) 20–30%, moderate (++) 50–60%, severe (+++) >80%. For the damage of mitochondria, 300 mitochondria were observed and the ratio of damaged mitochondria in 300 mitochondria was graded: normal (—) <10%, very mild (±) 10–20%, mild (+) 20–30%, moderate (++) 50–60%, severe (+++) >80%. For the lipid droplet number/five fields, normal (—) <10, very mild (±) 10–20, mild (+) 20–30, moderate (++) 50–60, severe (+++) >80. For the bundles, the ratio of distorted/five fields, normal (—) <10%, very mild (±) 10–20%, mild (+) 20–30%, moderate (++) 50–60%, severe (+++) >80%.

that mitochondria with highly electron-dense matrices and sproutlike structures, which were very similar in character to those of homozygous JVS mice (9), were frequently found (data not shown). In addition, the number of mitochondria was much higher than in the other mice.

Discussion

The present study demonstrated that mutation of *OCTN2* might be a risk factor for cardiomyopathy in JVS heterozygotes during aging, as predicted by our previous work (1). It is well known that carnitine deficiency results in mitochondria degeneration and lipid deposition through impaired energy metabolism in homozygous JVS mice (20). It is also known that heterozygous JVS mice have lipid deposits in myocytes (20). However, whether these changes progress during aging has never been tested in mice.

The results of this study partially confirmed that age-associated damage occurs in heterozygous mice as predicted by human study (1). Although the number of clinically recognizable cardiac hypertrophies was small, there was evidence that heterozygous mice developed metabolic cardiomyopathy during aging. First, similar morphological

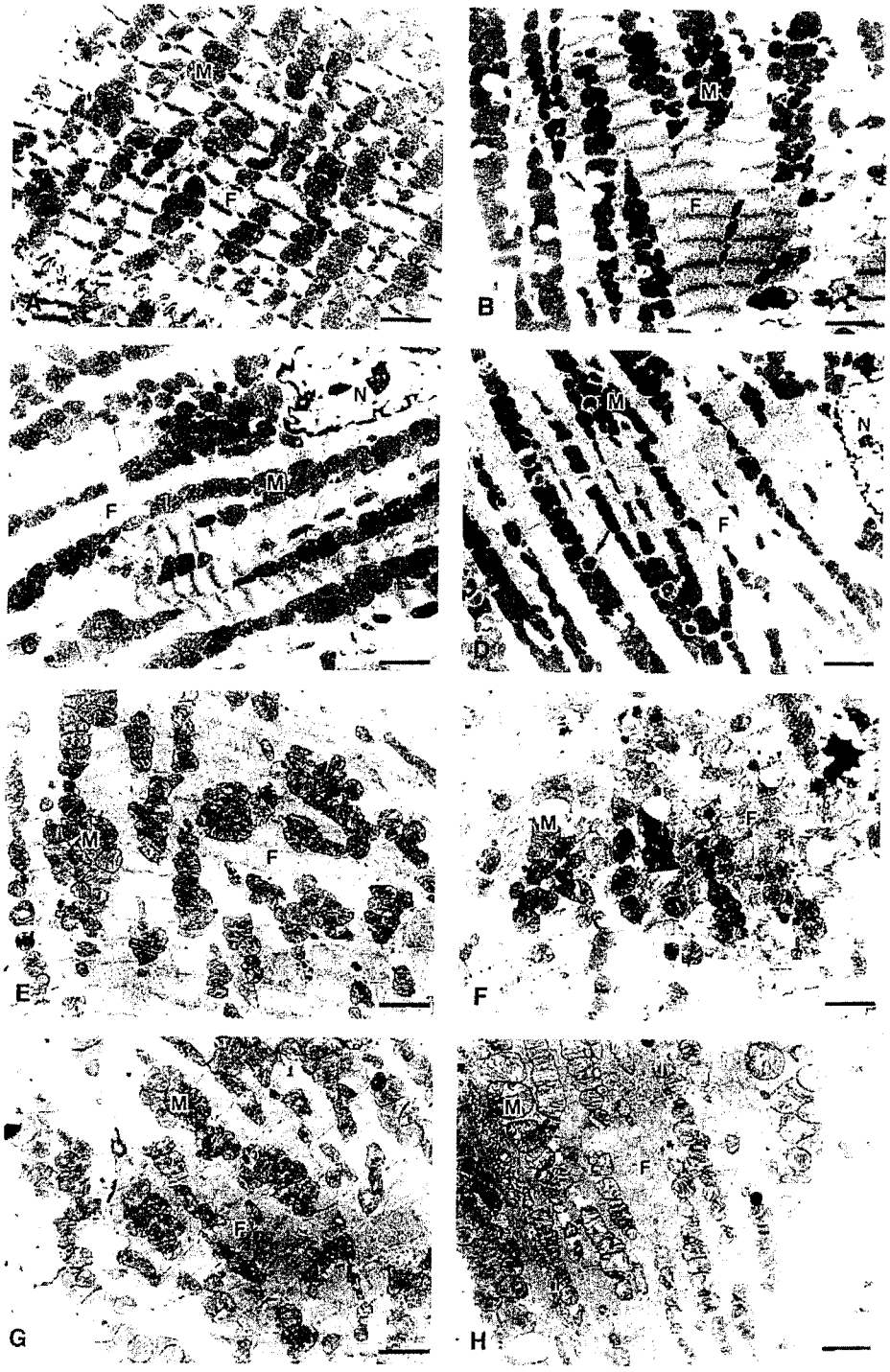

Figure 4. Electron microscopic photographs of myocytes of hearts from 1-year-old (**A–D**) and 2-year-old (**E–H**) mice. A large amount of lipid droplets (arrow), closely associated with the mitochondria, are seen in both male (**B**) and female (**D**) heterozygotes; however, in the age- and gender-matched control mice (**A** and **C**), there are no lipid droplets observed. For 2-year-old male (**F**) and female (**H**) heterozygotes, partially or completely digested swollen mitochondria (M) with disrupted cristae are markedly noted compared with male controls (**E**) and female controls (**G**), respectively. Moreover, regularly arranged mitochondrial cristae appear to be decreased mildly in 2-year-old controls (**E** and **G**) compared with 1-year-old controls (**A** and **C**). Scale bar = 2 μm. M = mitochondria; F = myofibrils; N = nucleus.

changes were found in diabetic rats that showed diabetic cardiomyopathy (21); second, the decreases in carnitine level in serum and cardiac tissue were comparable with those in diabetic rats with cardiomyopathy (21). These lines of evidence collectively suggest that JVS heterozygous mice had age-associated metabolic cardiomyopathy, but this was hard to detect as cardiac hypertrophy as indicated by a slight 6.6% increase in myocyte diameter. It should be noted, however, that other unknown factors may cause apparent cardiac hypertrophy, because only a small fraction of heterozygous carrier mice developed hypertrophy.

It is well known that impaired lipid and glucose metabolisms are risk factors for cardiomyopathy (14,22). In humans, the *OCTN2* mutation has been found in 0.5% of the screening population and is reported to be a significant risk factor for cardiomyopathy (1). No other risk factor related to cardiomyopathy with *OCTN2* mutation, including BMI and HDL, was found, except for the cholesterol level in men, but not in women, suggesting that increases in cholesterol levels may play only a subordinate role in cardiomyopathy in humans, if any. Likewise, in the study of mice, the cholesterol level was high in 2-year-old heterozygous mice, but not in 6-month-old or 1-year-old mice, which again is in accord with the notion that the *OCTN2* mutation acts directly on cardiomyopathy but is not mediated by cholesterol, BMI, or HDL. At present, however, the clinical implication of a male-specific increase in cholesterol level remains unknown. Further study is needed to clarify the mechanism.

Mitochondrial oxidative metabolism declines with age in many tissues. It has been reported that aging decreases the activity of electron transport chain complexes III (23) and IV (24) in interfibrillar populations of cardiac mitochondria (i.e., IFM), whereas oxidative phosphorylation in subsarcolemmal mitochondria remains unchanged (23,25). Aging-related decreases in fatty acid oxidation and complex IV activity were largely localized to IFM (26,27). In the present study, heterozygous mice had more IFM damage than control mice. Thus, in heterozygous mice, the genetic defect and aging work synergistically to accelerate degenerative processes relative to those of control mice.

Impaired oxidation of lipid substrates results in accumulation of long acyl-coA (28–30), which is known to inhibit pyruvate dehydrogenase in myocyte membranes and enhance calcium overloading, thereby leading to impairment of mitochondial integrity. It is well known that impaired mitochondrial integrity enhances electron leakage, leading to an increase in oxyradical production. Thus, heterozygous mice might be exposed to more oxidative stress than control mice as a result of a moderate reduction in carnitine levels in the interfibrillar population of cardiac mitochondria. It is also well established that mitochondria from aging tissues have increased oxidative stress even at basal levels (31,32). Thus, the combined effects of aging and a subtle molecular defect in carnitine homeostasis may accelerate the aging process in myocytes, leading to metabolic cardiomyopathy.

Carriers of autosomal recessive disorders are usually free from symptoms of the disease; however, the present study has demonstrated that increased cardiomyopathy with aging is a threshold trait for heterozygous carriers of pathological *OCTN2* mutations. This new evidence may suggest the possibility that some age-associated diseases may be attributable to heterozygous states of pathological mutations of other genes. This hypothesis is novel in terms of mechanism and must be studied further in future work. Determinations of molecular markers for cardiac hypertrophy and cardiomyopathy will give more information, which will be investigated in future studies.

In conclusion, although it is still premature to define the *OCTN2* mutation as a risk factor of cardiomyopathy, the heterozygous carrier state of *OCTN2* pathological mutation is shown to be a *possible* risk factor for age-associated cardiomyopathy as a threshold trait. This observation gives biological validity for the same phenomenon observed in humans obtained by epidemiological study (1), indicating that approximately 0.7–0.5% of the Japanese population may have a genetic risk factor for age-associated cardiomyopathy.

ACKNOWLEDGMENTS

This project was supported by grants-in-aid from the Ministry of Science, Culture and Sports of Japan (12557034 and 1270081) and Comprehensive Research on Aging and Health (H-11-Chojyu-010) from the Ministry of Health and Welfare of Japan.

We are greatly appreciative of Mr. Sasaki Yoshimitsu (Medical Research Center, Akita University School of Medicine, Akita, Japan) for his technical assistance. We are also grateful to Dr. Wang Yingjian (Hypromatrix, Inc., Millbury, MA) for helpful advice on the manuscript.

Address correspondence to Dr. Akio Koizumi, Department of Health and Environmental Sciences, Kyoto University School of Public Health, Kyoto 606-8501, Japan. E-mail: koizumi@pbh.med.kyoto-u.ac.jp

REFERENCES

1. Koizumi A, Nozaki J, Ohura T, et al. Genetic epidemiology of the carnitine transporter *OCTN2* gene in a Japanese population and phenotypic characterization in Japanese pedigrees with primary systemic carnitine deficiency. *Hum Mol Genet.* 1999;8:2247–2254.
2. Engel AG, Angelini C. Carnitine deficiency of human muscle with associated lipid storage myopathy: a new syndrome. *Science.* 1973;179: 899–902.
3. Roe C, Ding J. Mitochondrail fatty acid oxidation disorders. In: Scriver CR, Childs B, Beudet AL, et al., eds. *The Metabolic and Molecular Bases of Inherited Disease.* 8th ed. New York: McGraw-Hill; 2001:2297–2326.
4. Shoji Y, Koizumi A, Kayo T, et al. Evidence for linkage of human primary systemic carnitine deficiency with D5S436: a novel gene locus on chromosome 5q. *Am J Hum Genet.* 1998;63:101–108.
5. Tamai I, Ohashi R, Nezu J, et al. Molecular and functional identification of sodium ion-dependent, high affinity human carnitine transporter OCTN2. *J Biol Chem.* 1998;273:20,378–20,382.
6. Nezu J, Tamai I, Oku A, et al. Primary systemic carnitine deficiency is caused by mutations in a gene encoding sodium ion-dependent carnitine transporter. *Nat Genet.* 1999;21:91–94.
7. Chapoy PR, Angelini C, Brown WJ, Stiff JE, Shug AL, Cederbaum SD. Systemic carnitine deficiency—a treatable inherited lipid storage disease presenting as Reye's syndrome. *N Engl J Med.* 1980;303: 1389–1394.
8. Ghali JK III, Liao Y, Cooper RS. Left ventricular hypertrophy in the elderly. *Am J Geriatr Cardiol.* 1997;6:38–49.
9. Kuwajima M, Kono N, Horiuchi M, et al. Animal model of systemic carnitine deficiency: analysis in C3H-H-2° strain of mouse associated with juvenile visceral steatosis. *Biochem Biophys Res Commun.* 1991; 174:1090–1094.
10. Lu K, Nishimori H, Nakamura Y, Shima K, Kuwajima M. A missense mutation of mouse OCTN2, a sodium-dependent carnitine cotransporter, in the juvenile visceral steatosis mouse. *Biochem Biophys Res Commun.* 1998;252:590–594.

11. Horiuchi M, Kobayashi K, Yamaguchi S, et al. Primary defect of juvenile visceral steatosis (JVS) mouse with systemic carnitine deficiency is probably in renal carnitine transport system. *Biochim Biophys Acta.* 1994;1226:25–30.
12. Castelli WP, Wilson PW, Anderson K. Cardiovascular risk factors in the elderly. *Am J Cardiol.* 1989;63:H12–H19.
13. Kannel WB. Epidemiology of cardiovascular disease in the elderly: an assessment of risk factors. *Cardiovasc Clin.* 1992;22:9–22.
14. Kannel WB. Hypertension as a risk factor for cardiac events—epidemiologic results of long-term studies. *J Cardiovasc Pharmacol.* 1993; 21(suppl 2):S27–S37.
15. Koizumi T, Nikaido H, Hayakawa J, Nonomura A, Yoneda T. Infantile disease with microvesicular fatty infiltration of viscera spontaneously occurring in the C3H-H-2° strain of mouse with similarities to Reye's syndrome. *Lab Anim.* 1988;22:83–87.
16. Kuribayashi T. Spontaneously occurring hypertrophic cardiomyopathy in the rat. I. Pathologic features. *Jpn Circ J.* 1987;51:573–588.
17. Matsumori A, Kawai C. An animal model of congestive (dilated) cardiomyopathy: dilatation and hypertrophy of the heart in the chronic stage in DBA/2 mice with myocarditis caused by encephalomyocarditis virus. *Circulation.* 1982;66:355–360.
18. Warnick GR, Bederson J, Alberts JJ. Dextran sulfate-Mg^{2+} precipitation procedure for quantitation of high density lipoprotein cholesterol. *Clin Chem.* 1982;28:1379–1388.
19. Kaplan EL, Meier P. Non-parametric estimation from incomplete observations. *J Am Stat Assoc.* 1958;53:457–481.
20. Kaido M, Fujimura H, Ono A, et al. Mitochondrial abnormalities in a murine model of primary carnitine deficiency. Systemic pathology and trial of replacement therapy. *Eur Neurol.* 1997;38:302–309.
21. Malone JI, Schocken DD, Morrision AD, Gilbert-Barness E. Diabetic cardiomyopathy and carnitine deficiency. *J Diabetes Compl.* 1999; 13(2):86–90.
22. Kannel WB. The Framingham Study: its 50-year legacy and future promise. *J Atheroscler Thromb.* 2000;6:60–66.
23. Hoppel C, Cooper C. Studies on the nucleotide specificity of mitochondrial inner membrane particles. *Arch Biochem Biophys.* 1969; 135:184–193.
24. Hoppel CL, Tandler B, Parland W, Turkaly JS, Albers LD. Hamster cardiomyopathy. A defect in oxidative phosphorylation in the cardiac interfibrillar mitochondria. *J Biol Chem.* 1982;257:1540–1548.
25. Piper HM, Sezer O, Schleyer M, Schwartz P, Hutter JF, Spieckermann PG. Development of ischemia-induced damage in defined mitochondrial subpopulations. *J Mol Cell Cardiol.* 1985;17:885–896.
26. Edoute Y, van der Merwe E, Sanan D, Kotze JC, Steinmann C, Lochner A. Normothermic ischemic cardiac arrest of the isolated working rat heart. *Circ Res.* 1983;53:663–678.
27. Chen JC, Warshaw JB, Sanadi DR. Regulation of mitochondrial respiration in senescence. *J Cell Physiol.* 1972;80:141–148.
28. Corr PB, Snyder DW, Cain ME, Crafford WA Jr, Gross RW, Sobel BE. Electrophysiological effects of amphiphiles on carnine Purkinje fibers. Implications for dysrhythmia secondary to ischemia. *Circ Res.* 1981;49:354–363.
29. Corr PB, Sobel BE. Arrhythmogenic properties of phospholipid metabolities associated with myocardial ischemia. *Fed Proc.* 1983;42: 2454–2459.
30. Corr PB, Gross RW, Sobel BE. Amphipathic metabolities and membrane dysfunction in ischemia myocardium. *Circ Res.* 1984;55:135–154.
31. Richter C, Park JW, Ames BN. Normal oxidative damage to mitochondrial and nuclear DNA is extensive. *Proc Natl Acad Sci USA.* 1988;85:6465–6467.
32. Wallace DC. Mitochondrial defects in cardiomyopathy and neuromuscular disease. *Am Heart J.* 2000;139:S70–S85.

Received November 6, 2001
Accepted April 1, 2002
Decision Editor: John A. Faulkner, PhD